

This article appeared in a journal published by Elsevier. The attached copy is furnished to the author for internal non-commercial research and education use, including for instruction at the authors institution and sharing with colleagues.

Other uses, including reproduction and distribution, or selling or licensing copies, or posting to personal, institutional or third party websites are prohibited.

In most cases authors are permitted to post their version of the article (e.g. in Word or Tex form) to their personal website or institutional repository. Authors requiring further information regarding Elsevier's archiving and manuscript policies are encouraged to visit:

<http://www.elsevier.com/copyright>



Contents lists available at ScienceDirect

Journal of Physiology - Paris

journal homepage: www.elsevier.com/locate/jphysparis

Electrical neuroimaging of single trials to identify laterality and brain regions involved in finger movements

Rolando Grave de Peralta^{a,b,c,*}, Theodor Landis^b, Sara Gonzalez Andino^{a,b}

^aElectrical Neuroimaging Group, Geneva, Switzerland

^bGeneva University Hospital and Geneva University, Geneva, Switzerland

^cNeurodynamics Laboratory, Department of Psychiatry and Clinical Psychobiology, University of Barcelona, 08035 Barcelona, Catalonia, Spain

ARTICLE INFO

Keywords:

ELECTRA
Neuroprostheses
Oscillations
Electroencephalogram
Local field potential
Brain computer interface

ABSTRACT

Thought-controlled neuroprostheses could allow paralyzed patients to interact with the external world using brain waves. Thus far, the fastest and more accurate control of neuroprostheses is achieved through direct recordings of neural activity [Nicolelis, M.A., 2001. Actions from thoughts. *Nature* 409, 403–407; Donoghue, J.P., 2002. Connecting cortex to machines: recent advances in brain interfaces. *Nat. Neurosci.* 5 (Suppl.), 1085–1088]. However, invasive recordings have inherent medical risks. Here we discuss some approaches that could enhance the speed and accuracy of non-invasive devices, namely, (1) enlarging the spectral analysis to include higher frequency oscillations, able to transmit substantial information over short analysis windows; (2) using spectral analysis procedures that minimize the variance of the estimates; and (3) transforming EEG recorded activity into local field potential estimates (eLFP). Theoretical and experimental arguments are used to explain why it is erroneous to think that scalp EEG cannot sense high frequency oscillations and how this might hinder further developments. We further illustrate how non-invasive eLFPs derived from the scalp-recorded electroencephalogram (EEG) can be combined with robust, broad band spectral analysis to accurately detect (off-line) the laterality of upcoming hand movements. Interestingly, the use of pattern recognition to select the brain voxels differentially engaged by the explored tasks leads to sound neural activation images. Consequently, our results indicate that both research lines, i.e., neuroprosthetics and electrical neuroimaging, might effectively benefit from their mutual interaction.

© 2009 Elsevier Ltd. All rights reserved.

1. Introduction

In recent years we have witnessed impressive progresses in brain machine interfaces (BMI), i.e., controlling computers or other devices by brain waves. Using electrodes or tetrodes directly implanted into the brains, monkeys or severely paralyzed patients (Nicolelis, 2001; Craelius, 2002; Taylor et al., 2002) have been able to control mechanical devices or computers. However, rendering BMI useful to a larger population of patients implies reducing the medical risks inherent to direct brain implants as well as ensuring their long-term reliability.

An inexpensive and non-invasive alternative to long-term brain implants is the use of scalp EEG recordings. Still, EEG based BMI systems are far more inaccurate, slower and require long training periods before patients or normal volunteers learn to control their brain rhythms. This is because EEG signals represent the noisy

overlap of activity arising in diverse brain regions. Consequently, temporal (and thus spectral) features specific to diverse parallel processes arising in different brain areas are mixed on the same signal.

Recently, it has been shown that cortical recordings (ECoG) might provide a less invasive alternative to tetrodes based implants (Leuthardt et al., 2004). While still invasive, the temporal stability of ECoG signals seems to be easier to obtain. ECoG based neuroprosthetics provide accuracies superior to EEG based devices but still lower than tetrodes. Apparently, part of the ECoG success is based on the use of spectral features extracted from the range of oscillations (Leuthardt et al., 2004; Rickert et al., 2005) considered as non-measurable by scalp EEG (Schwartz et al., 2006). In addition, the spatial resolution of ECoG signals is finer than scalp measured signals that are spatially blurred by interfaces separating the cortex from the scalp, e.g., the skull, skin, and the cerebro-spinal fluids.

Here we show that there are techniques and approaches that can be used to close the gap between ECoG signals and EEG and therefore that there is potential for improvement in non-invasive neuroprosthetics. Recent developments in electrical neuroimaging

* Corresponding author. Address: Geneva University Hospital HUG, Rue Gabrielle Perret-Gentil 4, 1211 Geneva 14, Switzerland. Tel.: +41 223728323; fax: +41 223728333.

E-mail address: rolando.grave@hcuge.ch (R. Grave de Peralta).

(Grave de Peralta Menendez et al., 2000, 2004) allow the transformation of scalp recorded EEGs into estimates of local field potentials (eLFP). Transformation of EEG data into intracranial potentials allows us to unravel scalp signals, attributing to each brain area an estimate of its own temporal (spectral) activity. Thus non-invasively estimated LFP have the potential to be used as an alternative to control neuroprosthetic devices if they prove to compare in terms of speed and precision to ECoG signals (Mehring et al., 2003).

Here, we start with a brief description of the physiological basis of the different signals that can be used as control modalities in neuroprosthetics to better establish their similarities and differences. A discussion on the possibilities of scalp EEG to sense very high frequency oscillations and an introduction to the analysis techniques that better allow their reliable estimation follows. The main limitation of EEG signals, i.e., its low spatial resolution is proposed to be, at least partially, overcome by the use of non-invasive LFP estimation described in a separate section. Finally, the combination of techniques is illustrated in the analysis and classification of executed hand movements to show that decoding of motor intentions is possible using eLFP estimated from scalp EEG signals. It is further illustrated that using pattern recognition for voxel selection in electrical neuroimaging leads to reasonable activation images proving that both research lines might benefit from mutual interaction.

2. Methods

2.1. Different recording scales for neuroprosthetic control

Electrode technology for applied as well as basic neuroscience applications has significantly improved over recent years. We are today able to measure from a wide range spectrum of temporal frequencies, from “resting” or standing (DC) up to several kHz. This spectrum is commonly subdivided into two crude categories, near field intracellular or extracellular measurements and far field measurements.

Typical near-field extracellular measurements are performed by amplifying the potential difference between the microelectrode tip and a reference electrode located within a few millimeters. These recordings are usually broken into two components by filtering: the local field potential (LFP) corresponds to coherent high frequency changes in membrane potential (<300 Hz) associated with synaptic currents as well as other sources in cell aggregates, while the even higher frequency signal (300–10 kHz) consists mostly of multi-unit activity (MUA) resulting from action potentials (AP) in nearby neurons. MUA and LFP represent signals with widely different spatial extent: up to 100 μm for the single-unit signals, several hundreds of microns for the multi-unit signals, and several millimeters for the LFP.

LFPs are thought to represent extracellularly-recorded voltage fluctuations in the membrane potentials of a local neuronal population. LFPs originate from excitatory and inhibitory postsynaptic potentials (EPSP/IPSP), mainly as a result of action potential input. Postsynaptic potentials propagate much farther in space than MUA. Furthermore, because of their longer temporal duration EPSP and IPSP have a much higher chance to occur in a temporally overlapping manner than do the brief action potentials. Finally, EPSPs and IPSPs are displayed by many more neurons than are spikes because only a very small minority of neurons reaches the spike threshold at any instant in time. For these reasons, the contribution of action potentials to the local fields and especially to the scalp EEG is assumed negligible (13).

Depending on the location and size of the recording and reference electrodes, field potentials integrate neural activity over a

range of spatial scales: from the intracortical local field potential (LFP) to the intracranial electrocorticogram (ECoG) to the extracranial electroencephalogram (EEG). Additionally, magnetic field recordings can also be measured on the scalp using magnetoencephalography (MEG). These far field electrical recordings are similar to LFP in that they only contain significant low-frequency components. However, due to the amplitude attenuation by the skull and scalp and spatial filtering by volume-conduction in the brain, the spatial resolution of these recordings is considerably poorer than near-field recordings.

When dealing with neurophysiology in general and its concrete application to neuroprosthetics it is very important to keep in mind the differences between MUA and field potentials. While field potentials mainly reflect input to an area and local processing on it, MUA represent output from the area. Consequently, both measures encode different aspects of neural activity. Field potentials provide coarser although not necessarily less useful information about local processing than MUA.

2.2. On high frequency oscillations and fast EEG based BCIs

Due to the spatial filtering by volume-conduction the spatial resolution of EEG and MEG is poorer than that of near field recordings. Contrarily, to a widespread idea this does not imply that the frequency resolution of these techniques is different. In particular, it is erroneous to think that high frequency oscillations are not measurable by the scalp EEG. Some authors claim (Schwartz et al., 2006) that “... the large distance between the recording electrode and the underlying cortex allows capacitive effects of the tissue to shunt high-frequency currents more locally”. This assertion is wrong from both theoretical and experimental grounds. Already in 1957, Schwan and Kay showed that within biological tissues, the capacitive component of tissue impedance is negligible for frequencies below 1000 Hz. This experimental result is the basis of the quasi-static approximation (Plonsey and Heppner, 1967) on which all modeling of EEG and MEG relies upon. There is no solid theoretical reason to claim that scalp EEG recordings contain no spectral information above 70 Hz. What certainly holds true for all continuously recorded signals, i.e., LFP, ECoG and EEG, is that they exhibit a power-law frequency dependence with lower amplitudes for the higher frequencies. Further experimental validation to the absence of filtering effects by neural tissue comes from a recent study from Logothetis et al. (2007). These authors investigated the conductive properties of the gray matter in vivo concluding that gray matter behaves as an ohmic conductor, i.e., they showed that the cortex does not act as a frequency filter and does not impose different constraints on the propagation of electric signals of different temporal frequency. Notably, further results (Ikeda et al., 2002; Murakami and Okada, 2006) sustain the view that spiking activity might be detected from far field recordings of neural activity if enough synchronized across large enough populations. These results open a new window into EEG and MEG analysis and substantially encourage the exploration of fast oscillations.

Research on non-invasive neuroprosthetics has focused on relatively slow oscillatory activity (theta 4–8 Hz, alpha 8–12 Hz, beta 13–25 Hz and gamma 26–80 Hz). A pragmatic view of such oscillatory phenomena will reveal that there is no physical time for such oscillations to change, and therefore encode, information about highly dynamic processes. For instances, information relayed from one visual area to another only takes about 10 ms. If a particular oscillation is to carry this information, several cycles must be completed within this time. Some simple numerical computations will lead us to the conclusion that fast information encoding and transmission is most likely based on neural oscillations that are above 100 Hz also called epsilon oscillations.

Scalp EEG in newborns, in patients under anesthesia and in sleeping subjects is characterized by highly rhythmic oscillatory activity at low frequencies. On the other hand, the EEG of subjects that are in a relaxed state with eyes closed is generally characterized by strong occipital alpha oscillations. Opening the eyes induces a transition to a “more disorganized” less rhythmic state dominated by fast activity. Also, motor cortical activation during motor preparation and execution is related to the decrease of alpha and beta EEG sensorimotor rhythms. An increase in the alpha and beta rhythms occurs after movement termination. Intracortical recordings in epileptic patients (Crone et al., 1998) show that there is an inverse relationship between motor somatotopy and frequency of oscillations. The fastest rhythms are more focal and somato-topically organized than the slowest rhythms. Therefore, and somehow contrarily to the prevalent view, active and fast processing of stimuli does not produce the emergence of spatially synchronized rhythmic activity but rather a transition of the system towards very fast and less spatially organized dynamics.

Neuroscientific interest in neural oscillations above 100 Hz emerged relatively recently. Initially observed in rat's hippocampus during sleep (Buzsaki et al., 1992), they were coined ripples and are supposed to elicit the information transfer between the hippocampus and neocortex (Sirota et al., 2003). In rats (Barth, 2003) high frequency oscillations in the somato-sensory cortex of around 200 Hz are supposed to extract features of an object under exploration. In humans, evidence for very high frequency oscillations comes from intracranial recordings in epileptic patients (Brovelli et al., 2005; Edwards et al., 2005) and scalp EEG/MEG (Curio et al., 1994; Curio, 2000; Gonzalez et al., 2006). Interestingly, in a recent intracranial study (Brovelli et al., 2005), only the high gamma band activity (60–200 Hz) was able to distinguish the two different roles of the premotor cortex, that is, to separate motor intention from attention/memory. Also in humans, Canolty and co-workers (2006) showed coupling between the power of high frequency oscillations around 150 Hz and theta oscillation power and phase. The observed coupling varied with the behavioral task leading the authors to conclude that “cross-frequency coupling between distinct brain rhythms facilitates the transient coordination of cortical areas required for adaptive behavior in humans”. Simultaneous multi-unit activity (MUA) and local field potentials (LFP) in monkeys' inferior-temporal cortex revealed that LFP oscillations in the range 100–300 Hz are the ones that best correlate with MUA (Kreiman et al., 2006). Finally, several observations suggest that spontaneous very high frequency oscillations are not present in developing networks (Le Van Quyen et al., 2006). In rat pups, physiological ripple oscillations >140 Hz are observed in vivo in the hippocampus only after the end of the second postnatal week (Buhl and Buzsaki, 2005).

To summarize, previous experimental evidence indicates that: (1) very high frequency oscillations correlate better with MUA than low frequency oscillations; (2) very high frequency oscillations are more local than slow frequencies; (3) analysis based on very high frequency oscillations allows taking decisions on shorter analysis windows which is a mechanism more likely to appear in the brain when fast information transmission is needed. Consequently, restricting the analysis to the lower frequency bands might actually hinder progress in EEG in general and neuroprosthetics in particular. To facilitate progress in this area, it is essential to correctly analyze the weak high frequencies since they might often remain undetected if long analysis window and not-sensitive enough spectral analysis procedures are used.

2.3. Increasing the reliability of high frequency estimates by multitaper spectral analysis

The major problem with the estimation of high frequency oscillations is their low amplitude when compared to low frequency

oscillations. As discussed above, this is not a consequence of filtering properties of the tissues but rather appears to be a functional property of the neural circuits involved in the generation of the different brain rhythms. Apparently, the higher the frequency of the oscillation is the smaller the size of the population involved on its generation.

The practical consequence is that the amplitude of the high frequency oscillations measured at the scalp surface is of the order of the measuring error or might be even smaller. Consequently, not all spectral analysis procedures will provide correct estimates of these rhythms. Methods suited for the analysis of high frequency rhythms buried in noise should be able to reduce the variance of the estimates even to the expenses of lowering spectral resolution.

The multitaper method (Thomson, 1982; Bell et al., 1993) for spectral estimation (MTM) offers such possibility. The MTM is a non-parametric approach, i.e., it does not prescribe an a priori (e.g., auto-regressive) model for the process generating the time series under analysis. MTM attempts to reduce the variance of spectral estimates by computing a set of independent estimates of the power spectrum. The data are pre-multiplied by orthogonal tapers (discrete prolate spheroidal sequences) designed to minimize the spectral leakage due to the finite length of the data set. The final spectrum is computed by averaging over the ensemble of spectra yielding a lower variance estimate than do single-taper methods (Mitra and Pesaran, 1999). Within the concrete BCI context, a comparison between multitaper estimator and Welch methods (Mensh et al., 2004) showed slight advantages for multitaper estimates but the differences did not reach statistical significance. Noteworthy, Mensh and co-workers demonstrated that better classification is achieved when gamma band and slow cortical potentials are combined with respect to the classification obtained when only slow potentials are used. This observation emphasize the need to widely explore the whole frequency range of oscillations to better detect those able to discriminate between cognitive tasks rather selecting narrow frequency bands which were defined on historical rather than physiological basis.

2.4. A simple measure for feature selection: the discriminative power

The specific functional role of different brain rhythms is not yet fully understood. Rhythms are context dependent and the same frequency band might play different roles depending on its neural origin and functional characteristics (e.g., evoked or induced). For these reasons it is difficult to predict which particular frequency bands are better to discriminate, as desired for neuroprosthetic applications, two or more mental tasks. Even the conventional definition of the bounds of the frequency bands is often challenged by experimental results.

It is therefore desirable to have a procedure that automatically detects the frequencies (or bands) that provide the better between class discrimination. In what follows we briefly describe the concept of discriminative power, a rather intuitive and fast approach to feature selection that we have been successfully using in the past.

To define the DP measure we depart from the idea that if the amplitude of a certain range of neural oscillations carries specific information about the subject functional/cognitive state, then the distributions of the power of this oscillation (the power spectral density, PSD) should be different for different tasks. This yields a measure graded between 0 and 100, with zero representing complete overlap between both PSD distributions (no discrimination between tasks is possible) and 100 representing the perfect separation between them. The DP provides an estimate of how many trials can be unambiguously classified on the basis of a given frequency at a single electrode. For details see Gonzalez et al. (2006).

2.5. Non-invasive estimation of LFPs

One major aspect limiting the application of the EEG as a control modality in neuroprosthetics is its low spatial resolution. This resolution could be potentially improved if we were able to disentangle the superposition of signals observed at the scalp attributing this activity back to its neural origin. This necessarily passes by the solution of an inverse problem. Contrarily to inverse problems linked to other neuroimaging modalities, e.g., fMRI, MRI, PET, the EEG inverse problem lacks a unique solution. Constraints need to be introduced to reduce the space of all possible potential distributions within the brain able to explain one recorded scalp map. Constraints can be imposed at several levels. In what follows we describe how constraints derived from the physics of the problem can be set on the type of sources able to generate measured maps. These constraints constitute the theoretical basis of a method allowing a non-invasive although coarse estimation of LFP from scalp recorded EEG data. Simulation studies and preliminary experimental findings indicate that it can produce trustworthy estimates of the temporal structure of LFP. These estimates made possible to produce brain images reflecting the brain areas in which oscillatory activity (OA) is modulated in response to stimulus type and cognitive states. Thanks to its non-invasiveness, this method has been used to decode the behavioral or cognitive state of healthy humans with excellent accuracy (Gonzalez Andino et al., 2007). In what follows we briefly sketch the mathematical foundations of this approach. For further details, the interested reader is referred to Grave de Peralta Menendez et al. (2004).

Poisson equation describes the relationship between scalp surface EEG and the (primary) current density vector (J^p) under the quasi-static approximation of Maxwell equations. Assuming a simple head model with unitary conductivity (a similar result is obtained for piecewise constant conductivity) and denoting by G the Green function, it can be written in any of the two following forms:

$$V(r) = \int_V \nabla \cdot J^p(r_v) G(r, r_v) \quad (\text{P1})$$

$$\nabla \cdot \nabla V = \nabla \cdot J^p \quad (\text{P2})$$

where V denotes the electrical potential at scalp site r and r_v stand for points that belong to the brain volume. As for any vector field, the primary current density vector can be written as the sum of a solenoidal vector field, plus an irrotational vector field, plus the gradient of a harmonic function, i.e., $J^p = \nabla \phi + \nabla \times \mathbf{A} + \nabla H$. Substituting this expression into Eq. (P1) demonstrates that only the irrotational part ($\nabla \phi$) can produce the potential V (i.e., EEG measurements). Importantly this result holds whatever the conductivity pattern is. Furthermore, feeding the irrotational part $\nabla \phi$ into (P2) proves that the scalar function ϕ (potential) has the same Laplacian, and thus, the same sources and sinks as V . In simpler words we can say that ϕ and V are equal up to an arbitrary harmonic function. This source model has been named ELECTRA (Grave de Peralta Menendez et al., 2000).

Concurrent experimental evidence was provided by Plonsey (1982) who stated that “the fields measured do not even arise from (the primary sources) J but rather from secondary sources only. These secondary sources, in turn, depend on both the electrical field and the interfaces, and hence are related to $\nabla \cdot J$ and the geometry”.

In summary, the non-invasive estimation of LFP relies on a physical truth concordant with existing experimental evidence. Since only a few EEG measurements are usually available, there is no sense in looking for sources that cannot generate the measured data. This introduces a strong constraint, since the space of arbitrary current distributions explaining the measurements is re-

duced to that of irrotational currents. This space is still infinite, i.e., the solution is not yet unique. However, the original inverse problem, i.e., the estimation of the current density vector (3 components) at each brain voxel is transformed into the estimation of a potential function (a single value) at each brain voxel.

To definitely single out the solution, we use a regularization operator (Grave de Peralta et al., 2001) based local auto-regressive average (LAURA) model. It consists in a set of local averages (i.e., weights that sum one) regressing the activity in one point as a weighted combination of the activity in the other points. Importantly, the weights are selected to follow the behavior of the potential of known sources (e.g., potential of the dipole) which are irrotational everywhere except at a single point.

2.6. Applying non-invasively estimated LFP to a simple visuo-motor task

In what follows we show how these ideas can be combined within a very simple experiment to provide fast and accurate classification of hand response laterality. The goal of this analysis is to show that the combination of techniques described above allows classifying impending hand movements using very short analysis windows. Noteworthy, speeded visuo-motor reaction time tasks as the one considered here, are common in real life situations such as driving a car or playing a computer game and should not be ignored within neuroprosthetic research. In such tasks, a visual cue (e.g., crossroad) serves as a warning signal that compels a motor reaction.

Subjects and Task: Twelve healthy, right-handed subjects (six women, 21–27 years) were tested. The task consisted of fixating a central cross and of responding as fast as possible with one index finger to a black dot. Each subject was tested in two blocks. In all blocks, stimuli appeared every 5–6 s in random order either in the left or in the right visual field. The central cross, serving as the warning signal, preceded the stimulus by 3–4 s and remained visible until the end of the response. In one block, responses were made with the index finger of the left hand, in the other block with the index finger of the right hand. Responses were assessed with a response key device with a temporal precision of <1 ms. Hands of the subjects rested over the response key and head was stabilized by means of a head and chin rest. Each subject was tested in 120 trials per block.

EEG recording and preprocessing. EEG data were recorded using the Geodesic Sensor Net (Tucker, 1993), which arranges 129 Ag/AgCl electrodes in a tension structure that insures the sensors are distributed evenly across the head surface. The EEG signals were amplified with a high input-impedance (Zin 200 MW) Net Amps dense-array amplifier (Electrical Geodesics, Inc.). The data were recorded with a 0.1–500 Hz analog band-pass filter and digitized with a 16-bit analog-to-digital converter. The data were collected with the common electrode located at the nasion and the reference electrode located at the vertex. Visual inspection was used to identify and reject trials contaminated by movement artefacts if falling within the analysis window. EEG epochs of length equal to each subject fastest response were selected. This period is the most likely to include motor preparation while excluding actual execution of the movement likely to induce spurious classification based on electromyographic activity. Since no EMG data was recorded during the experiment a rather strict criterion was used for artefact rejection after which 77 trials (out of 120) we kept on average (over subjects) for posterior analysis.

Analysis procedure for each subject. For each trial selected for analysis, the EEG traces recorded on the scalp were transformed into intracranial estimates of LFP as described in Section 2.5. These estimates were obtained at 4024 discrete pixels distributed on the grey matter of the MNI brain. The computation of the lead field

matrix and the regularization parameter followed the procedure described in Grave de Peralta and Andrino (2008).

Once the LFP traces were computed for every single brain voxel (eLFP), the following steps were applied: (1) single trial based computation of power spectral density (PSD) for the pre-selected analysis window; (2) splitting the data into a learning (initial half of trials) and a test set (remaining trials); (3) feature selection based on the training set; and (4) computation the percentage of correctly decoded trials in the test set. Specific implementation details are given below.

2.6.1. Single trial based computation of PSD

The eLFP were transformed to the frequency domain using the multitaper method (seven sleeping data tapers). Each temporal analysis window was multiplied by each of the tapers and the Fourier components were then computed via FFT. The PSD was computed by taking square of the modulus of these complex numbers corresponding to frequencies from 0 (DC) to half of the frequency sampling, i.e., 250 Hz.

2.6.2. Splitting the data into a learning and a test set

The whole data set was divided into two halves: (1) a learning set composed of the first half of trials and used to detect the most discriminative features and (2) a test set formed by the second half of trials that is used to evaluate the classification.

2.6.3. Feature selection over the learning set

To select the most relevant features, i.e., the patterns of oscillatory activity that characterize each cognitive/motor task we relied on the discriminative power measure described above (Gonzalez et al., 2006). The discriminative power (DP) was computed for all voxels and frequencies over the single trials that belonged to the learning set. As in Gonzalez et al. (2006) we computed two different definitions of features (oscillatory patterns): (F1) the PSD at all voxels for the most relevant frequency as identified by the DP and (F2) the best 150 PSD sorted according to their DP combining all sensors and frequencies in the range 0-half of frequency sampling.

2.6.4. Measuring decoding accuracy

The accuracy of the decoding was defined as the percentage of trials on the test set that were correctly attributed to their original class by a multivariate pattern recognition algorithm known as linear support vector machine (Hastie et al., 2001). The particular implementation used was the linear OSU-SVM implemented in the Matlab toolbox OSU-SVM (Ma, J., Zhao, Y., Ahalt, S. Matlab toolbox OSU-SVM 3.0, available at http://www.eleceng.ohio-state.edu/~maj/osu_svm). All (hyper) parameters were set to their default values. The percentage of correctly decoded trials in the test set was computed using a leave-one-out cross-validation. Leave-one-out (LOO) cross-validation is a method to estimate the predictive accuracy of the pattern recognition algorithm. Given n trials in the test set, the pattern recognition is trained on $(n - 1)$ trials, and then is tested on the trial that was left out. This process is repeated n times until every trial in the dataset has been included once as a cross-validation instance. The results are averaged across the n trials. Notably, the LOO estimate is an almost unbiased estimate of the expected generalization error (Chapelle et al., 2002).

3. Results

Our aim was to discriminate which hand (left or right) was engaged in a simple manual response task using a time window of duration equal to the subject's fastest response. Table 1 describes the obtained classification rates for the two sets of features used. On the basis of these results we can conclude that accurate predic-

Table 1

Percentage of correct classification of laterality of upcoming movements based on non-invasive estimates of local field potentials. Classification is obtained for a time window of duration equal to the subject's fastest response using two different spectral features (PS): the best 150 features after ranking by the DP (F1) and the best feature for each frequency (F2).

Subject	Analysis window (ms)	Best frequency (Hz)	eLFP (F1/F2)
1	183	30	100/94
2	102	41	98/91
3	225	48	90/78
4	166	175	100/88
5	175	145	100/96
6	144	31	91/88
7	102	40	93/73
8	222	95	99/95
9	158	132	98/98
10	191	170	93/74
11	147	70	98/86
12	131	111	98/92
Average	147	85	97%

tion of hand movement laterality based on spectral features can be done accurately and rapidly enough to reproduce each subject's fastest response. A similar analysis to the one described above using amplitude selected features in the temporal domain for both EEG and estimated LFPs leads to classification rates barely above chance. Fig. 1 shows a single subject mean ERPs aligned by the motor response for the left hand movements over three electrodes, one over the fronto-central line and the two others placed closer to C3 and C4. The ERP traces are superimposed on the mean scalp map obtained for the time point where C4 reaches its maximum. The map shows the classical pattern characteristic of left hand movements with maxima over electrodes covering the motor cortex contralateral to the moved hand. However, the ERP traces show little sign of lateralized readiness potentials. It is therefore not

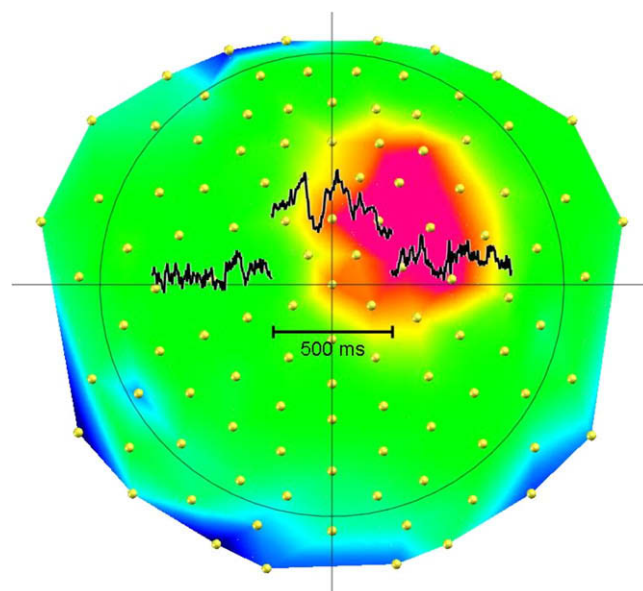


Fig. 1. Single subject mean ERPs (left hand movement) over contacts lying above motor cortex and ERP map for the time at which amplitude is maximal at electrodes near C4. The maximum is reached 5 ms before movement onset. ERP data were obtained by aligning trials to the onset of motor response. The ERP traces over three electrodes either placed closer to C3 and C4 or over the fronto-central line (near FCz) are superimposed on the mean scalp map obtained when the contact near C4 reaches its maximum. Note that the map maximum lies over electrodes covering the motor cortex contralateral to the moved hand but the ERP traces show little sign of lateralized readiness potential.

surprising that classification based on amplitude derived features fail in this case which is very likely due to the speeded nature of the hand movements that leaves little time for motor preparation.

Fig. 2 shows the logarithm of the mean spectral power computed using the multitaper method on contacts lying near C3 and C4 for six of the subjects considered in this study. Both left and right hand movements are shown. For subjects (d), (b) and (e) the spectral power in the range 60–200 Hz is clearly higher for left hand movements than for right hand movements near C4, i.e., the electrode covering the right motor cortex. In contrast, similar power spectrum is observed for both hand movements near C3. If the differences observed in this study were due to simple EMG contamination, then the opposite pattern should be observed. The electrodes closer to the moved hand should pick up more EMG activity and therefore power for left hand movements should be higher than power for right hand movement near C3. Note also that the situation is inverted, i.e., right hand movements lead to stronger power spectrum over the contralateral contact (C3) than left hand movement for subjects (a) and to some extent (c). In

addition, the spectra exhibit the typical $1/f$ law characteristic of neural activity (note the logarithmic scale) rather than the relatively flat spectrum typical of EMG activity.

Fig. 3 shows the average over subjects of the maximum discriminative power over all brain voxels. These plots provide information on the LFP oscillations that best serve to decode left from right hand intentions in view of their task-related modulation. The highest discriminative power, over subjects with more than 60% of the samples decoded, is observed for the gamma band (40 Hz). However, the discriminative power remains high for the very high frequency oscillations with a drop in discrimination observed after 200 Hz.

The two insets in Fig. 4 depict the overall distribution over subjects of the 150 voxels that better discriminate the laterality of movements irrespective of the frequency band where they discriminate. The voxels are further divided into two groups (two insets) according to the sign of the difference in the mean spectral power for both movements, i.e., power left hand – power right hand. The topmost inset (Fig. 4a) represents then the part of the

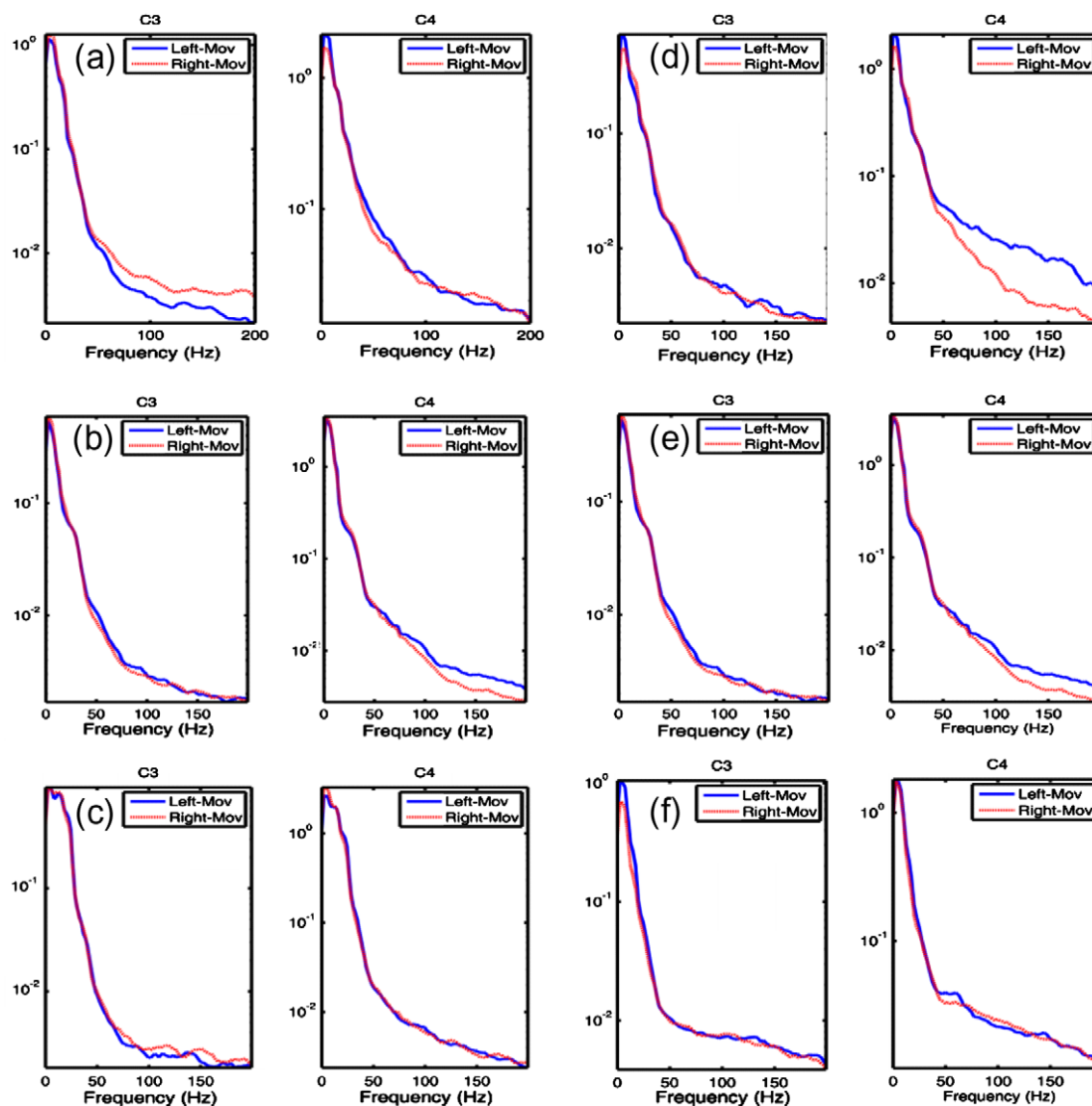


Fig. 2. Mean power spectrum for 6 of the 12 subjects considered in this study when left (blue) or right (red) hand movements are performed. The spectrum is computed for the analysis window considered here, i.e., from visual stimulus onset up to the fastest reaction time for each subject and depicted for electrodes closer to the locations of C3 and C4. The spectra were computed using the multitaper method and represented in a logarithmic scale. Both, the $1/f$ shape of the spectra and the lateralization of the effects to the contralateral rather than ipsilateral hemisphere suggest that high frequency effects are of neural origin rather than EMG contamination.

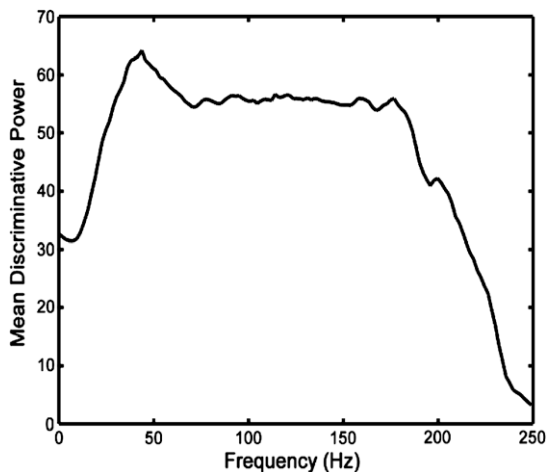


Fig. 3. Mean (over subjects) discriminative power (DP) vs. frequency. Mean over subjects of the best DP observed over the whole solution space. A peak in the discrimination is observed at gamma band but discrimination is still high for frequencies up to 180 Hz where a drop is observed.

150 voxels where OA power for the frequency at which the voxel discriminate is higher for left than right hand responses. The lower inset (Fig. 4b), depicts the part of the 150 most discriminative voxels where spectral power was higher for right hand responses. To create this summary image over subjects we first created individual images where we assigned a value of one to voxels belonging to the best 150 features used for classification. Voxels that appear repeatedly (i.e., the same voxel that discriminates at more than one frequency) were considered only once. To summarize information over subjects we summed the individual images to code in color the amount of subjects displaying the specific effect at each area. In all panels, results are surface-rendered onto a canonical brain using the MRICRO software.

4. Discussion

The results of our analysis suggest that a combination of individual feature selection over a broad band of frequencies and the non-invasive estimation of LFPs provide physiologically interpretable results and good decoding accuracy over very short analysis windows. Best classifying spectral features are localized over motor and premotor areas with the laterality distribution expected on this task. The best classifying voxels are confined to the premotor cortex, a region implicated in visually controlled movements. Voxels at the dorsal premotor cortex (PMd) provide consistent discrimination between conditions over subjects. This result agrees with studies (Hoshi and Tanji, 2004) in non-human primates indicating that the PMd area is involved in integrating information about which arm to use and the target to be reached. Taken as a whole, our results indicate that scalp recorded EEG signals contain relevant information about neural functioning coded in terms of oscillations that allows perfect and fast differentiation on at least this simple motor task. What is probably more important, creating a neural activation image that relies on pattern recognition applied to features selected in the frequency domain leads to neurophysiologically interpretable results which are not necessarily identical to conventional inverse solution images. A similar finding has been reported for the case of fMRI images (Kamitani and Tong, 2004), where pattern recognition actually increases the spatial resolution of functional images when compared to conventional statistical processing. While further research is certainly needed on this issue, it nonetheless confirms that functional neuroimaging might benefit from analysis techniques regularly used within neuroprosthetic research.

We have here provided theoretical and experimental evidence to refute claims that VHFO are not measurable at the scalp surface. This aspect is very important since invasive recordings of neural activity within and outside the scope of neuroprosthetic have revealed a role for very high frequency oscillations in neural

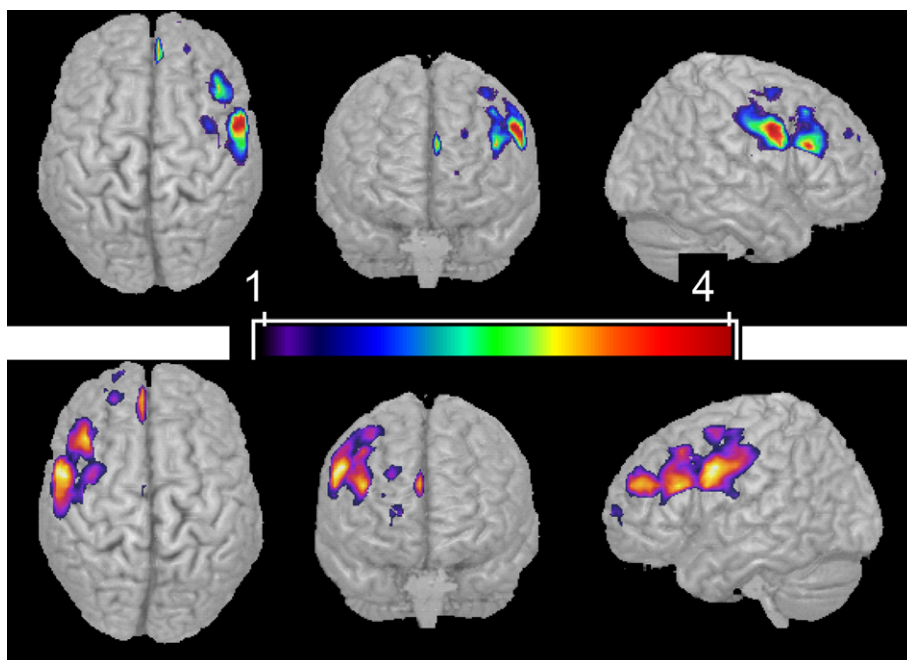


Fig. 4. Brain voxels that better discriminate on average (over subjects) between right and left hand movements (all frequencies confounded). Spectral power is computed for the LFP estimated at each brain voxel using a multitaper method. The DP is used to determine frequencies and voxels where the probability densities (PD) of spectral power over trials differ the most between both classes of movements. The topmost inset (a) represents the part of the 150 voxels where OA power for the frequency at which the voxel discriminate is higher for left than right hand responses. The lower inset (b) depicts the part of the 150 most discriminative voxels where spectral power was higher for right hand responses.

function. After our initial study using the same dataset described here, two newer studies have addressed the importance of oscillations above 100 Hz for neuroprosthetics and found no such relationship. Both, methodological and experimental reasons might explain the differences.

In the first of the studies Waldert et al. (2008) used EEG and MEG to decode the direction of center-out hand movements. Both, the experiment and the goal of the analysis differ from ours. Frequencies encoding movement laterality are not necessarily the same as those coding for movement direction. A second study (Bai et al., 2007) failed to disclose influences of very high frequency oscillations on a self-paced task where sequences of keys had to be pressed. The EEG signals in later study were low-pass filtered at 100 Hz using a third-order Butterworth filter which prevent observation of VHFO.

Our initial study on VHFO (Gonzalez et al., 2006) already revealed interesting inter-individual differences in the range of frequencies that provide the best decoding. In fact, gamma or high gamma band oscillations provide the best decoding for half of the subjects and VHFO for the other half. Indeed, in a preliminary study (unpublished data) we have assessed the decoding power of very high frequencies in a self-paced finger tapping task. Interestingly, oscillations above 100 Hz provide the best decoding when the same hand is used for key presses within a block but not when the left and right finger responses are alternated within a block. Since every subject performed both tasks within the same session and using the same fingers and hands it cannot be a consequence of EMG contamination but very likely a reflect of motor adaptation (learning). Furthermore, since this task is self-paced, the possibility that visuo-motor integration processes could explain the emergence of VHFO is ruled out. These results are more consistent with a physiological role of the VHFO and the existence of consistent inter-individual and across-tasks variability. The most likely explanation for divergences in results is that the range of frequencies that better discriminate between different tasks is exquisitely sensitive to the nature of the task itself. For instances, while the ERP analysis of the visuo-motor data considered here, showed consistent lateralization of motor responses over contralateral motor cortex, the free choice selection of most discriminant frequencies done by the DP measure did not revealed slow frequencies that should be expected if readiness potentials were the only functional marker of this task. While further research is needed to understand why high frequency oscillations rather than slow potentials are more discriminative in this example, it nevertheless illustrates the importance of broad spectral exploration for the selection of relevant features for neuroprosthetic and more importantly for the whole field of EEG analysis.

5. Conclusions

Here, we have discussed some approaches that could contribute to enhance the capabilities of non-invasive neuroprosthetic systems based on scalp EEG recordings. In particular, we have shown that wide band spectral analysis combined with non-invasively estimates of field potentials provide excellent decoding results on at least a simple task, suggesting new alternatives for the development of direct non-invasive neuroprosthetic systems. Issues such as the precise role of very high frequency oscillations or the best approach to obtain unique better estimates of Local Field Potentials deserve further study.

Acknowledgments

This work was supported by European Project FP6-IST-027140 (BACS) and the COST Action BM0601 "NeuroMath". This paper only

reflects the authors' views and funding agencies are not liable for any use that may be made of the information contained herein.

References

- Bai, O., Lin, P., Vorbach, S., Li, J., Furlani, S., Hallett, M., 2007. Exploration of computational methods for classification of movement intention during human voluntary movement from single trial EEG. *Clin. Neurophysiol.* 118, 2637–2655.
- Barth, D.S., 2003. Submillisecond synchronization of fast electrical oscillations in neocortex. *J. Neurosci.* 23, 2502–2510.
- Bell, B.M., Percival, D.B., Walden, A.T., 1993. Calculating Thomson's spectral multitapers by inverse iteration. *J. Comput. Graph. Stat.* 2, 119–130.
- Brovelli, A.L.J., Kahane, P., Boussaoud, D., 2005. High gamma frequency oscillatory activity dissociates attention from intention in the human premotor cortex. *NeuroImage* 28, 154–164.
- Buhl, D.L., Buzsaki, G., 2005. Developmental emergence of hippocampal fast-field "ripple" oscillations in the behaving rat pups. *Neuroscience* 134, 1423–1430.
- Buzsaki, G., Horvath, Z., Urioste, R., Hetke, J., Wise, K., 1992. High-frequency network oscillation in the hippocampus. *Science* 256, 1025–1027.
- Canolty, R.T., Edwards, E., Dalal, S.S., Soltani, M., Nagarajan, S.S., Kirsch, H.E., Berger, M.S., Barbaro, N.M., Knight, R.T., 2006. High gamma power is phase-locked to theta oscillations in human neocortex. *Science* 313, 1626–1628.
- Chapelle, O., Vapnik, V., Bousquet, O., Mukherjee, S., 2002. Choosing multiple parameters for support vector machines. *Mach. Learn.* 46, 131–159.
- Craelius, W., 2002. The bionic man: restoring mobility. *Science* 295, 1018–1021.
- Crone, N., Miglioretti, D., Gordon, B., Lesser, R., 1998. Functional mapping of human sensorimotor cortex with electrocorticographic spectral analysis. II. Event-related synchronization in the gamma band. *Brain* 121, 2301–2315.
- Curio, G., 2000. Linking 600-Hz "spikelike" EEG/MEG wavelets ("sigma-bursts") to cellular substrates: concepts and caveats. *J. Clin. Neurophysiol.* 17, 377–396.
- Curio, G., Mackert, B.M., Burghoff, M., Koetitz, R., Abraham-Fuchs, K., Harer, W., 1994. Localization of evoked neuromagnetic 600 Hz activity in the cerebral somatosensory system. *Electroencephalogr. Clin. Neurophysiol.* 91, 483–487.
- Donoghue, J.P., 2002. Connecting cortex to machines: recent advances in brain interfaces. *Nat. Neurosci.* 5 (Suppl.), 1085–1088.
- Edwards, E., Soltani, M., Deouell, L.Y., Berger, M.S., Knight, R.T., 2005. High gamma activity in response to deviant auditory stimuli recorded directly from human cortex. *J. Neurophysiol.* 94, 4269–4280.
- Gonzalez Andino, S.L., Grave de Peralta, R., Khateb, A., Pegna, A.J., Thut, G., Landis, T., 2007. A glimpse into your vision. *Hum. Brain Mapp.* 28, 614–624.
- Gonzalez, S.L., Grave de Peralta, R., Thut, G., Millan, J.d.R., Morier, P., Landis, T., 2006. Very high frequency oscillations (VHFO) as a predictor of movement intentions. *NeuroImage* 32, 170–179.
- Grave de Peralta Menendez, R., Gonzalez Andino, S.L., Morand, S., Michel, C.M., Landis, T., 2000. Imaging the electrical activity of the brain: ELECTRA. *Hum. Brain Mapp.* 9, 1–12.
- Grave de Peralta Menendez, R., Murray, M.M., Michel, C.M., Martuzzi, R., Gonzalez Andino, S.L., 2004. Electrical neuroimaging based on biophysical constraints. *NeuroImage* 21, 527–539.
- Grave de Peralta Menendez, R., Gonzalez, S.L., Lantz, G., Michel, C.M., Landis, T., 2001. Noninvasive localization of electromagnetic epileptic activity. I. Method descriptions and simulations. *Brain Topogr.* 14, 131–137.
- Grave de Peralta, R.G., Andino, S.L.G., 2008. Non-invasive estimates of local field potentials for brain-computer interfaces: theoretical derivation and comparison with direct intracranial recordings. In: Bozovic, V. (Ed.), *Medical Robotics*. I-Tech Education and Publishing, Vienna.
- Hastie, T., Tibshirani, R., Friedman, J.H., 2001. *The Elements of Statistical Learning: Data Mining, Inference, and Prediction*. Springer, New York.
- Hoshi, E., Tanji, J., 2004. Functional specialization in dorsal and ventral premotor areas. *Prog. Brain Res.* 143, 507–511.
- Ikeda, H., Leyba, L., Bartolo, A., Wang, Y., Okada, Y.C., 2002. Synchronized spikes of thalamocortical axonal terminals and cortical neurons are detectable outside the pig brain with MEG. *J. Neurophysiol.* 87, 626–630.
- Kamitani, Y., Tong, F., 2004. Pattern recognition of orientation-selective fMRI signals in the human visual cortex. *J. Vis.* 4, 186.
- Kreiman, G., Hung, C., Quiñero, R., Kraskov, A., Poggio, T., DiCarlo, J.J., 2006. Object selectivity of local field potentials and spikes in the macaque inferior temporal cortex. *Neuron* 49, 1–13.
- Le Van Quyen, M., Khalilov, I., Ben-Ari, Y., 2006. The dark side of high-frequency oscillations in the developing brain. *Trends in Neurosciences Nature and Nurture in Brain Development and Neurological Disorders* 29, 419–427.
- Leuthardt, E.C., Schalk, G., Wolpaw, J.R., Ojemann, J.G., Moran, D.W., 2004. A brain computer interface using electrocorticographic signals in humans. *J. Neural Eng.* 2, 1741–2552.
- Logothetis, N.K., Kayser, C., Oeltermann, A., 2007. In vivo measurement of cortical impedance spectrum in monkeys: implications for signal propagation. *Neuron* 55, 809–823.
- Mehring, C., Rickert, J., Vaadia, E., Cardoso de Oliveira, S., Aertsen, A., Rotter, S., 2003. Inference of hand movements from local field potentials in monkey motor cortex. *Nat. Neurosci.* 6, 1253–1254.
- Mensh, B.D., Werfel, J., Seung, S., 2004. BCI competition 2003 – data set Ia: combining gamma-band power with slow cortical potentials to improve single-trial classification of electroencephalographic signals. *IEEE Trans. Biomed. Eng.* 51, 1052–1056.

- Mitra, P.P., Pesaran, B., 1999. Analysis of dynamic brain imaging data. *Biophys. J.* 76, 691–708.
- Murakami, S., Okada, Y., 2006. Contributions of principal neocortical neurons to magnetoencephalography and electroencephalography signals. *J. Physiol.* 575, 925–936. doi:10.1113/jphysiol.2006.105379.
- Nicolelis, M.A., 2001. Actions from thoughts. *Nature* 409, 403–407.
- Plonsey, R., Heppner, D.B., 1967. Considerations of quasistationarity in electrophysiological systems. *Bull. Math. Biophys.* 29, 657–664.
- Plonsey, R., 1982. The nature of sources of bioelectric and biomagnetic fields. *Biophys. J.* 39, 309–312.
- Rickert, J., Oliveira, S.C., Vaadia, E., Aertsen, A., Rotter, S., Mehring, C., 2005. Encoding of movement direction in different frequency ranges of motor cortical local field potentials. *J. Neurosci.* 25, 8815–8824.
- Schwan, H.P., Kay, C.F., 1957. Capacitive properties of body tissues. *Circ. Res.* 5, 439–443.
- Schwartz, A.B., Cui, X.T., Weber, D.J., Moran, D.W., 2006. Brain-controlled interfaces: movement restoration with neural prosthetics. *Neuron* 52, 205–220.
- Sirota, A., Csicsvari, J., Buhl, D., Buzsaki, G., 2003. Communication between neocortex and hippocampus during sleep in rodents. *PNAS* 100, 2065–2069.
- Taylor, D.M., Tillery, S.I., Schwartz, A.B., 2002. Direct cortical control of 3D neuroprosthetic devices. *Science* 296, 1829–1832.
- Thomson, D.J., 1982. Spectrum estimation and harmonic analysis. *Proc. IEEE* 70, 1055–1096.
- Tucker, D.M., 1993. Spatial sampling of head electrical fields: the geodesic sensor net. *Electroencephalogr. Clin. Neurophysiol.* 87, 154–163.
- Waldert, S., Preissl, H., Demandt, E., Braun, C., Birbaumer, N., Aertsen, A., Mehring, C., 2008. Hand movement direction decoded from MEG and EEG. *J. Neurosci.* 28, 1000–1008. doi:10.1523/jneurosci.5171-07.2008.